A review on oxide/metal/oxide thin films on flexible substrates as electrodes for organic and perovskite solar cells

Mihaela Girtan, Beatrice Negulescu

Optical Materials X xxx (xxxx) 100122

Contents lists available at ScienceDirect

Optical Materials X

journal homepage: www.journals.elsevier.com/optical-materials-x

Journal Cover Image

Invited Article

A review on oxide/metal/oxide thin films on flexible substrates as electrodes for organic and perovskite solar cells

Mihaela Girtan [a, *], Beatrice Negulescu [b]

[a] Photonics Laboratory, (LPhiA) E.A. 4464, SFR Matrix, Université d'Angers, Faculté des Sciences, 2 Bd Lavoisier, 49000, Angers, France
[b] GREMAN, UMR 7347, Université de Tours, CNRS, Parc de Grandmont, 37200, Tours, France

ARTICLE INFO

Keywords:
Flexible organic solar cells
Flexible perovskite solar cells
Oxide/metal/oxide flexible electrodes
Semi-transparent and tandem solar cells
Polymers
PET substrates
CH3NH3PbI3
P3HT:PCBM
IMI
NAN
DMD
ZAZ
OMO
TAT

ABSTRACT

This paper gives an overview on the recent advances on the oxide/metal/oxide (OMO) on flexible plastic substrates and their applications as electrodes for organic and perovskite solar cells. The morphological, optical and electrical characteristics of different type of OMO electrodes such as: IMI (ITO/Metal/ITO), ZAZ (ZnO/Au or Ag/ZnO), NAN (NiO/Ag/NiO), TAT (TiO_2/Ag/TiO_2), DMD (MoO_3/Ag/MoO_3, SnO_2/Ag/SnO_2 etc.) collected from literature are presented and analyzed. This analysis allows to identify the most promising materials and the best choices in term of layers thickness for obtaining high quality electrodes with high transmission coefficients, high electrical conductivity and low roughness. The solar cells performances using these three layer electrodes are compared with those of the same devices in the classical configuration using ITO or FTO on plastic substrates as bottom electrodes or Au and Ag silver as top electrodes. It results a mean variation of about ±15% in efficiency performances in function of materials or technologies. The organic or perovskites solar cells classical configuration is: glass or PET substrate/ITO or FTO bottom electrodes/active layers/Au or Ag top electrodes. In the new configuration the usual bottom or top electrodes are replaced with OMO electrodes. Hence the new configurations are: 1) PET substrate/OMO bottom electrode/active layers/Au or Ag top electrode, or 2) PET substrate/ITO or FTO bottom electrode/active layers/OMO This last configuration lead to the developed of a new class of tandem or semi-transparent flexible solar cells based on organic or perovskite materials, which performances are very competitive with those deposited on classical configurations. The advantage of OMO are their mechanical, electrical and optical stability and their reduced cost by the reduction or suppression of some rare materials such as ITO.

1. Introduction

Flexible electronics and photonics devices on lightweight substrates are the new technologic and scientific challenges for the next generation applications [1–11]. There are many reasons for the development of the technologies in this direction. First, the reduction of device weight is of major importance in the energy reduction consumption and of crucial importance in the case of spatial applications. The second reason is related to the raw material crisis and the scarcity of some materials involved in the device fabrication such as In, Ge, Sb, rare earth etc. [12]. Moreover, polymers flexible substrates can be prepared form cellulose but also from the already too much existing plastic wastes such as PET. PET – Poly(Ethylene Terephthalate), as glass, can be easily melt and reuse many times without and no any industrial production from primary resources would be necessary [13]. The new generation solar cells fabrication processes are also much more economic and the energy production consumption is reduced.

In the case of monocrystalline and polycrystalline silicon solar cells, the front electrodes are generally silver paste grid. These electrodes mask a part of the active surface area of the cell, reducing the number of the photo carriers that would be possible to generate. In the case of thin films solar cells, the front electrodes are transparent conducting electrodes based generally on ITO (Tin doped Indium Oxide) [14–17], FTO (Fluor doped Tin Oxide) [18], IZO or AZO (Indium or Aluminum doped Zinc Oxide) [19–25]. These oxide semiconductor materials, if they are highly doped conduct to a degeneration of the semiconducting character and they become what we call "degenerate-semiconductors" having excellent conducting properties close to the one of metallic materials [26]. There are few materials belonging to this class of transparent conductors, as generally increased doping rises the conductivity but reduces the transmission and vice-versa. Hence, to achieve achieve

* Corresponding author.
E-mail address: mihaela.girtan@univ-angers.fr (M. Girtan).

https://doi.org/10.1016/j.omx.2021.100122
Received 5 September 2021; Received in revised form 7 October 2021; Accepted 11 October 2021

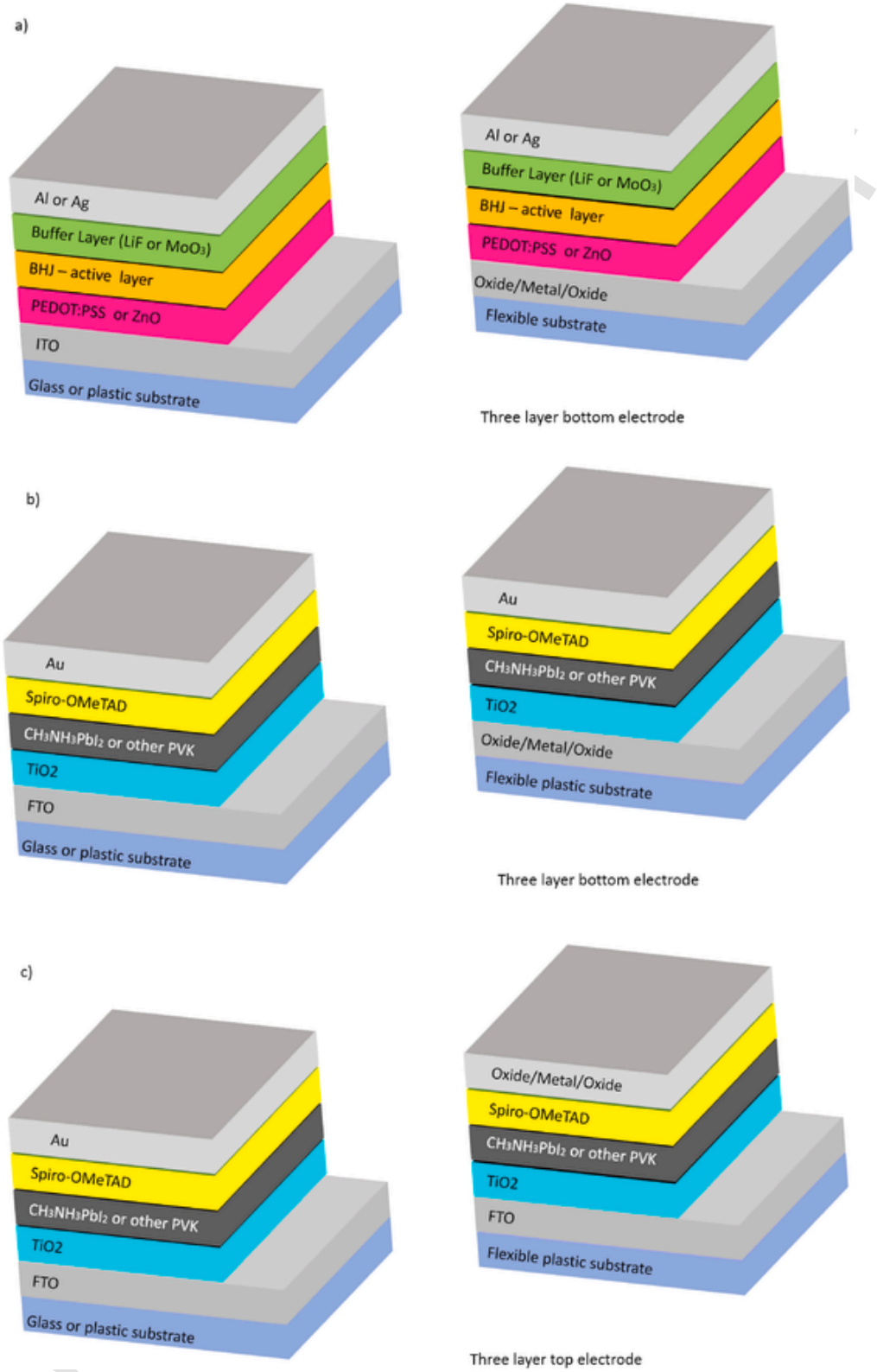

Fig. 1. On the left side are given the classical architectures and on the right side the new architectures with oxide/metal/oxide (OMO) as electrodes for a) OPV solar cells b) PVK solar cells with OMO electrodes as bottom electrode c) PVK solar cells with OMO electrodes as top electrode.

both high electrical conductivity and high optical transparency in the visible domain is difficult. An alternative to these transparent conducting oxides are also few transparent conducting polymers such as PEDOT:SS [27,28], graphene, carbon nanotubes or silver nanowires [29]. Not all these materials are suitable for deposition on flexible polymer substrates, as an issue related to the elasticity of the structure is the mechanical stability of the electrodes. The oxide thin films are brittle and crack after few successive bends. The conducting polymers or the nanostructured carbon or silver electrodes are mechanically compatible with the flexible substrates. However, they can be concerned by other

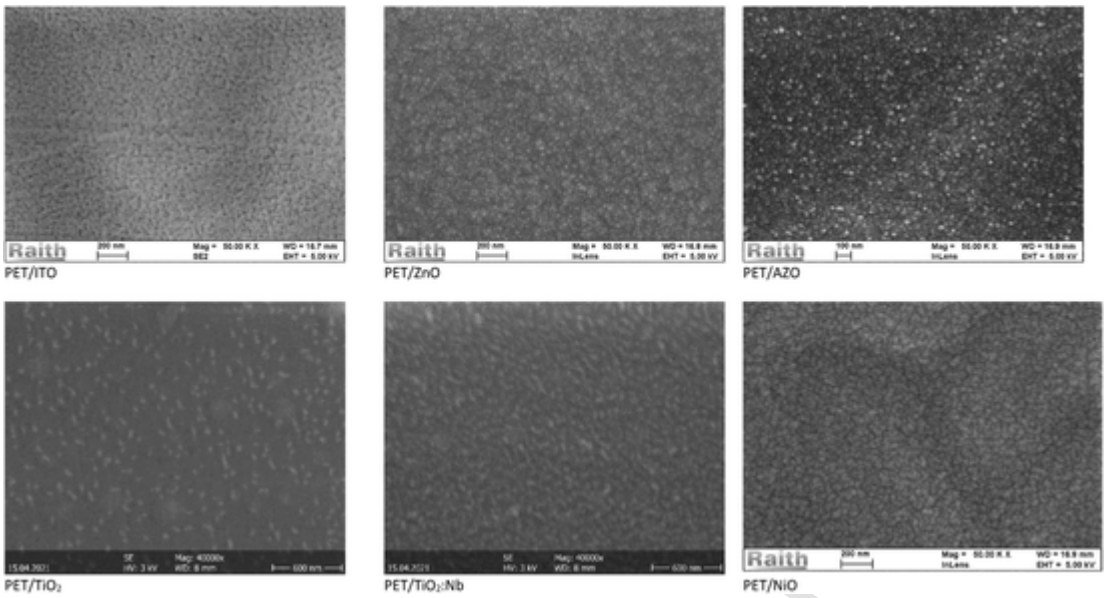

Fig. 2. SEM micrographs of transparent oxide films on PET substrates.

Table 1
Summary of the root mean square (RMS) and average (RA) roughness values of the oxide top layer of the multilayer structures oxide/metal/oxide deposited on PET substrates.

Multilayer structure on PET substrate	Thickness (nm)	RMS values (nm)	RA values (nm)	Reference
ITO/Ag/ITO	20/7/20	3.0	1.9	[33]
ITO/Au/ITO	20/8/20	1.9	1.5	[33]
ITO/Ag/Au/ITO	20/7/7/20	2.4	1.8	[33]
ITO/Ag/ITO	40/9/40	2.0	–	[35]
ITO/Ag co Cu/ITO	40/5/40	0.36	–	[35]
ZnO/Ag/ZnO	25/8/25	10.8	8.5	[33]
ZnO/Au/ZnO	25/8/25	5.7	4.6	[33]
ZnO/Ag/ZnO	30/14/30	4.2	–	[34]
AZO/Au/AZO	40/7/40	2.8	2.2	This work
TiO_2/Ag/TiO_2	24/8/37	13.1	10.3	[36]
TiO_2/Au/TiO_2	30/7/30	5.7	4.0	This work
TiO_2/Au/TiO_2	30/10/40	8.3	–	[37]
TiO_2:Nb/Ag/TiO_2:Nb	34/8/42	26.5	20.7	[36]
NiO/Ag/NiO	42/8/72	6.8	5.4	[36]
NiO/Ag/NiO	35/11/35	1.7	–	[38]
Bi_2O_3/Au/Bi_2O_3	120/7/120	2.7	1.2	This work
MoO_3/Ag/MoO_3	40/10/40	8.5		[39]

Table 2
Contact angle wetting properties of the oxide top layer of the multilayer structures oxide/metal/oxide compared to single oxide layer.

Interlayer	Thin film layer	Thickness (nm)	CA values (deg)	Reference
Au	ITO	45	92	[40]
	ITO/Au/ITO	45/7/45	60	[40]
	AZO	40	109	[40]
	AZO/Au/AZO	40/7/40	60	[40]
	TiO_2	30	78	[40]
	TiO_2/Au/TiO_2	30/7/30	70	[40]
	Bi_2O_3	35/11/35	84	[40]
	Bi_2O_3/Au/Bi_2O_3	120/7/120	82	[40]
Ag	TiO_2	28	55	[36]
	TiO_2/Ag/TiO_2	28/8/37	95	[36]
	TiO_2:Nb	28	70	[36]
	TiO_2:Nb/Ag/TiO_2:Nb	34/8/42	91	[36]
	NiO	63	93	[36]
	NiO/Ag/NiO	42/8/72	96	[36]

problems such as their chemical stability, or difficulties on large scale manufacturing. An alternative which overcome the problems of the mechanical fragility and conserve the high chemical stability, high transparency and electrical conductivity is the oxide/metal/oxide heterostructure. This multilayer structure combine all the required qualities and despite the increased number of layers the total electrode thickness is reduced. Indeed, if the usual thickness of the ITO, FTO, AZO single films ranges between 150 nm and 250 nm, in the multilayer structures only 20–40 nm thick oxide layers are used in combination with 7–8 nm metallic interlayer. Hence, the total thickness of the multilayer electrodes varies from 47 nm to 88 nm (20/7/20 minimum to 40/8/40 maximum). Therefore, if we compare the quantity of ITO needed for a single layer (about 150–160 nm) with the quantity of ITO used in a there layer electrode ITO/metal/ITO (20/7/20) it is easy to observe a reduction by 4 of the ITO quantity necessary for the fabrication of the multilayer electrodes. The reduction of the single layer electrode thickness under 120 nm would induce a dramatically decrease of the electrical conductivity due to the well-known semiconductors dimensional effect. This reduction by four of the material quantity is necessary and quite imposed, because ITO is a material intensively used in the fabrication of all today electronic and optoelectronic devices (computers, mobile phones, panels, light emitting diodes, solar cells etc.) and the depletion of the very limited resources of Indium on Earth will soon conduct to a crisis in this area, if a replacement or consumption reduction solutions are not found. Alternative indium free multilayer oxide/metal/oxide structures, studied since now are: ZnO/Metal/ZnO, AZO/Metal/AZO, TiO_2/Metal/TiO_2, NTO/Metal/NTO, (NTO meaning Niobium doped Titanium oxide), NiO/Metal/NiO, Bi_2O_3/Metal/Bi_2O_3, MoO_x/Metal/MoO_x, SnO_2/Metal/SnO_2, the metallic interlayer being generally: Au or Ag.

In this paper we present a selection of the main properties of these oxide/metal/oxide multilayer structures used as bottom or top electrodes in organic (OPV) and perovskite (PVK) solar cells deposited on flexible substrates. The performance of the devices using these new electrodes are compared with their performances in the classical configuration using ITO or FTO single layer electrodes on the same flexible substrates.

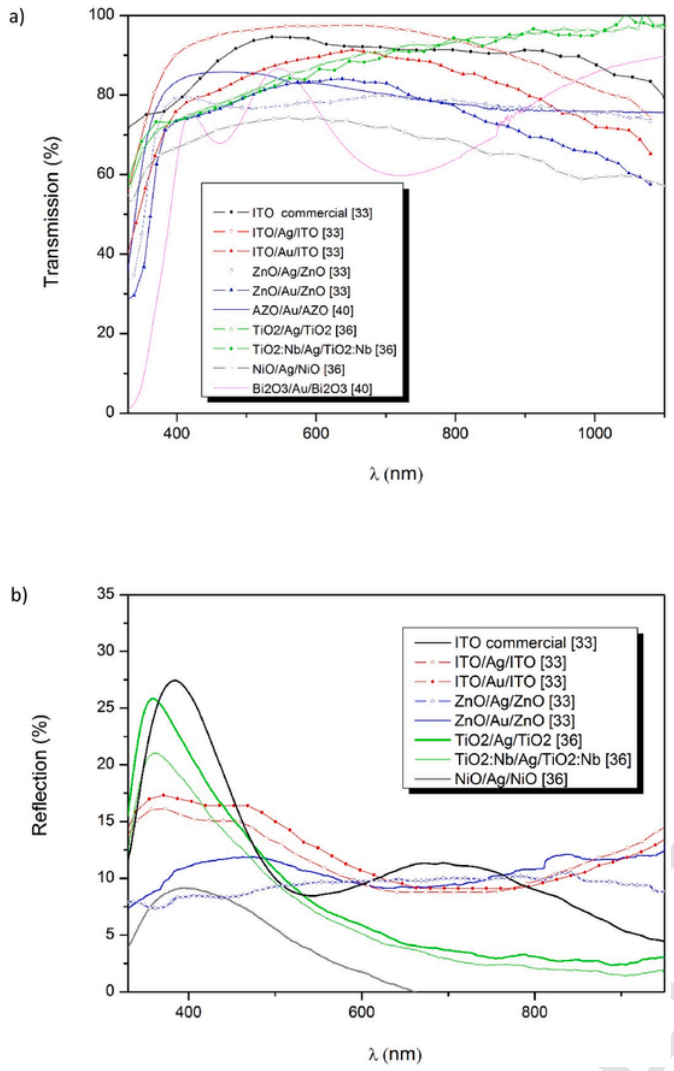

Fig. 3. a) Transmission spectra for different series of oxide/metal oxide thin films b) reflection spectra for the same samples.

2. Fabrication and structural characterization of the oxide/metal/oxide electrodes

The most employed method for oxide/metal/oxide (OMO) electrodes manufacture is DC or RF magnetron sputtering. The oxide layers can be deposited from the corresponding oxide materials target or from metallic targets in reactive atmosphere. The metallic interlayer is deposited in neutral conditions, generally under Argon atmosphere. The deposition by sputtering has several advantages such as a very good control of deposition parameters and a very high reproducibility. The rate of deposition is acceptable (between few nanometers by minute up to few hundreds nanometers in function of the deposition system power and materials nature) and the method can be used at industrial scale for deposition on surfaces of several meters square at room temperature. Other methods used are: e-beam evaporation, thermal evaporation and self-assembling. For e-beam evaporation and self-assembling the reproducibility and the parameter control are good, but the rate of deposition is low. The thermal evaporation is a less reproducible method and the thin films deposition can become difficult in the case of some oxides due to the very high melting point of these materials (1843 °C for TiO_2, 1975 °C for ZnO, 1955 °C for NiO, 1630 °C for SnO_2) but can be used for the deposition of MoO_3 (795 °C), Bi_2O_3 (817 °C), Au (1064 °C) and Ag (962 °C).

The full device preparation for OPV and PVK perovskite varies slightly from a laboratory to another. Generally the active layers are deposited from solutions by spin coating or Doctor Blade method, different additive or buffer layers are used to increase the solar cells efficiency. For the classical electrode configuration, with ITO on glass substrates, in 2021 the world record for OPV solar cells was of 18% and the detailed fabrication procedure of theses solar cells is given in Ref. [30]. For PVK solar cells, the world record to date is of 25.6% for a solar cells using as active material the FAPbI3 [31], and FTO on glass as transparent electrode.

The classical and new architectures, using oxide/metal/oxide bottom or top electrodes, of organic and perovskite solar cells are given in Fig. 1.

From technological point of view, in order to obtain a good transparency and a high electrical conductivity of the oxide/metal/oxide multilayer structures, the thickness of oxide and metallic layers should be optimized and chosen carefully. Especially the thickness of the metallic inter-layer is critical. The optimal value of this thickness is generally of about 7 or 8 nm. If the metallic film is too thin the obtained electrodes are not enough conducting and if this layer is too thick the electrode is not enough transparent and the reflection coefficient is too high. Of course, in both cases the solar cells performances will be reduced. The excellent mechanical performances to bending of these electrodes comparing to single oxides ITO or FTO are due to the ductility of the metallic films.

The optimization from optical and electrical point of view of the multilayer architecture can be done not only experimentally, but also theoretically by ellipsometry modelling [32].

The morphology of the transparent oxide films on PET substrates is given, as an example, for a series of materials used for oxide/metal/oxide electrodes in Fig. 2. Electrode's flatness is an important parameter, especially in the case of bottom electrodes, as roughness can conduct to short-circuit into the device. Table 1 gives the values extracted from literature completed with some new data, of the roughness of multilayer structures deposited on plastic substrates.

As a general remark, the roughness of oxide/metal/oxide films is higher when the deposition is done on PET substrates than on glass [33,34]. Also, as can be remarked from Table 1, the roughness is increased in the three layer structures using silver interlayer compared with those using gold. In the case of structures using Ag, the reduction of the roughness can be done by the deposition of a second different metallic layer (Au) as suggested by Girtan in Ref. [33] for ITO/Ag/Au/ITO (RMS 1.2 nm on glass and 2.4 nm on PET) vs. ITO/Ag/ITO (RMS 2.8 nm on glass and 3 nm on PET), or by co-evaporation of a second metal (Cu) by Spinelli et al.: ITO/Ag/Cu/ITO on PET (RMS 0.36 nm) vs. ITO/Ag/ITO on PET (RMS 2.02 nm) [35].

The contact angle measurements (see Table 2) reveal the fact that, comparing to single oxide thin films, the contact angles decrease for the multilayer oxide/metal/oxide structures with Au interlayer metallic thin films and increase for the ones with Ag. These results are in agreement with the observations concerning the roughness measurements.

3. Optical and electrical oxide/metal/oxide thin films transparent electrodes characteristics

The quality of transparent conducting electrodes is generally appreciate in function of their figure of merit. There are two figures of merit (FOM) generally used: the figure of merit of Fraser and Cook (1) and the figure of merit of Haake (2), which formulas are given below:

$$F_{TC} = \frac{\mathrm{T}}{R_{sq}} \quad (1)$$

$$\Phi_{TC} = \frac{T^{10}}{R_{sq}} \quad (2)$$

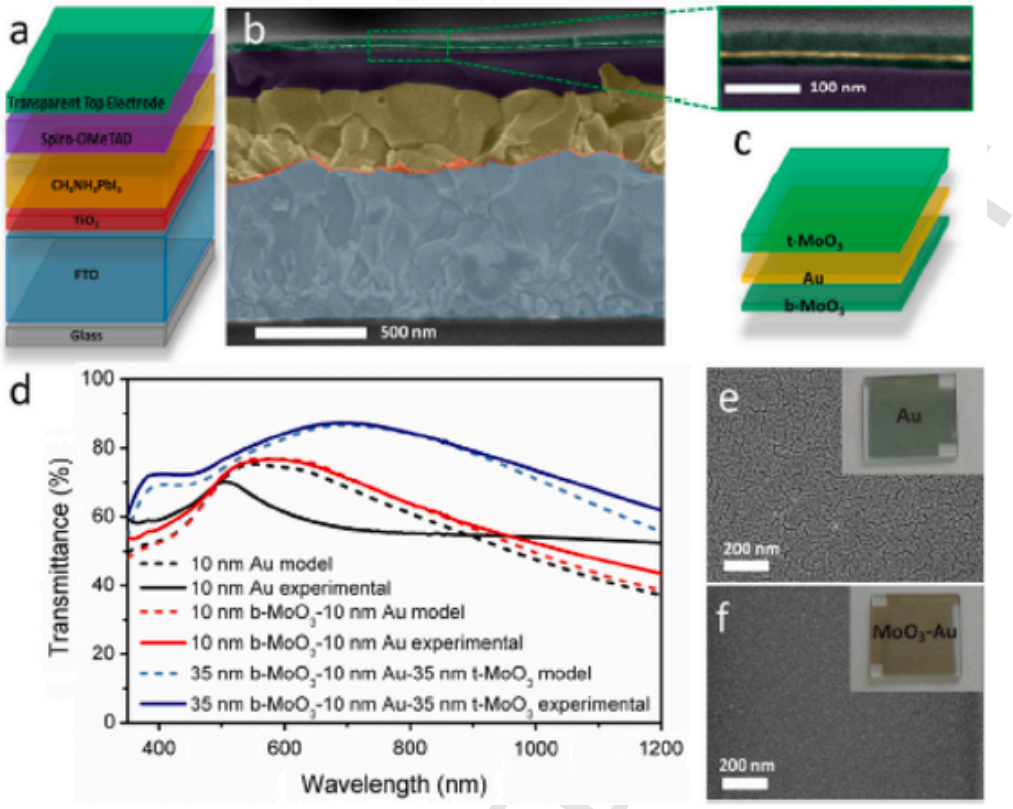

Fig. 4. a) The architecture of a CH3NH3PbI3 perovskites solar cell on glass substrate using a MoO_3/Au/MoO_3 multilayer structure as top electrode b) SEM image in cross section of a complete device c) Enlarged view of the multi-layer top electrode and schematic of its structure d) transmission spectra of the MoO_3/Au/MoO_3 the top electrode (e) SEM image of Au film f) SEM image of the bottom MoO3/Au film and inset of the two samples. Reprinted with permission from Nano Energy 13 (2015) 249 [41].

here T being the transmission coefficient and R_{sq} the sheet resistance.

The transmission spectra of different multilayer structures oxide/metal/oxide are given in Fig. 3 in comparison with the transmission spectra of transparent ITO commercial thin films used for the preparation of solar cells and other optoelectronic devices.

Also, as an example, the SEM micrographs and the transmission spectra of a MoO_3/Au/MoO_3 multilayer structure used as top electrode in the architecture of a CH3NH3PbI3 perovskites solar cell on glass substrate are given in Fig. 4.

It can be remark from Figs. 3 and 4, that the optical transmission of oxide/metal/oxide layers, with few exceptions, is generally lower, around 80% vs. 90–95% for ITO commercial films. Higher transmittance coefficients or comparable were remarked (see Table 3) for ITO/Metal/ITO (IMI) multilayer structures when the metallic interlayer do not exceed 7 or 8 nm. Moreover, from the reflection spectra, it could be noticed that the reflection coefficients for ITO/Ag/ITO and ITO/Au/ITO are smaller than those of commercial ITO: 15% vs. 25% at 400 nm.

Hence, from optical point of view, we can mention that the optical properties of IMI thin films electrodes are comparable or even better than those of usual ITO. Other good candidates are ZnO/Metal/ZnO structures with high transmission and low reflection coefficients. TiO_2/Metal/TiO_2 layers, have high transmittance but also they are more reflecting, hence their use can be more interesting as back reflecting electrodes combined with another oxide/metal/oxide electrode for the manufacturing of semitransparent or multi-junctions solar cells.

The combined electrical and optical data collected from literature are summarized in Table 3 for the films presented previously. The values marked with a star (*) correspond to the values calculated using the formulas (1) and (2) when these respective values were not given directly by the authors. The values of FOM allow to identify faster the series of materials having the most promising properties. However, it should be mentioned that their absolute value shouldn't be taken "ad literam" or as unique criteria because the calculated values of FOM take into account the transmission coefficient only for a unique value of the wavelength (here $\lambda = 550$ nm) which could be not relevant in we take into account the absorption domain of solar cells. For the multilayers structures deposited on plastic substrate, the highest values of Haake FOM are obtained for ITO/metal/ITO films, followed by equivalent values for the structures using ZnO, AZO, NiO, TiO_2, TiO_2:Nb and MoO_3. According to a first study results [40], films of Bi_2O_3/Au/Bi_2O_3 present poorer qualities, but it possible that these characteristic could be improved by an optimization of the deposition parameters.

From electrical characteristic point of view, a major difference of multilayer structures, comparing to the classical ITO or FTO electrode, is that one that the electrical conductivity of oxide/metal/oxide is stable in function of temperature and will not vary during the device functioning as is the case of ITO of FTO films [42].

4. Organic and perovskite solar cells on flexible substrates using oxide/metal/oxide electrodes

The potential of oxide/metal/oxide and among them, the ones of IMI (ITO/Metal/ITO) and ZMZ (ZnO/Metal/ZnO) electrodes on plastic substrates and their advantages compared to classical ITO, was mentioned for the first time in 2012 by Girtan in Ref. [33]. In 2014, P. Kubis et all realized for the first time a flexible module using IMI sputtered stack as transparent electrode (see Fig. 5).

The IMI electrode characteristics were ITO (40 nm)/Ag (10 nm)/ITO (40 nm) having a transmission coefficient more than 85% at 550 nm and a sheet resistance of 7.7 Ω/sq, which is 7 time less than the sheet resistance of usual single ITO films on PET (47.4Ω/sq) [43]. The

Table 3
Fraser and Cooke and Haake figures of merit respectively, for the multilayer structures oxide/metal/oxide deposited on PET substrates, calculated at 550 nm transmittance.

Substrate	Multilayer structure	Thickness (nm)	R_{sq} (Ω/)	T(%) λ = 550 nm	Figure of merit ($10^{-3}\Omega^{-1}$) λ = 550 nm		Reference
					Fraser - Cook	Haake	
PET	ITO/Ag/ITO	20/7/20	25	97	39	29	[33]
PET	ITO/Au/ITO	20/8/20	16.7	88	53	16	[33]
PET	ITO/Ag/Au/ITO	20/7/7/20	6.7	84	127	24	[33]
PET	ITO/Ag/ITO	40/10/40	7.7	88	114[a]	36[a]	[43]
PET	ITO/Ag/ITO	-/9/-	11.3	70	61.9[a]	2.5[a]	[35]
PET	ITO/Ag/Cu/ITO	40/5/65	16	78.5	49[a]	5.5[a]	[35]
PET	ZnO/Ag/ZnO	25/8/25	16.7	77	46	4	[33]
PET	ZnO/Au/ZnO	25/8/25	16.7	82	49	8	[33]
PET	ZnO/Ag/Au/ZnO	25/8/9/25	10	83	83	15	[33]
PET	ZnO/Ag/ZnO	30/14/30	8	76.5	96[a]	8.6	[34]
PEN	ZnO/Ag/ZnO	40/10/20	8.61	80	93[a]	12.5[a]	[44]
PET	AZO/Au/AZO	40/7/40	–	–	32	8	[40]
PET	TiO_2/Ag/TiO_2	24/8/37	1014	84	0.8	0.2	[36]
PET	TiO_2/Au/TiO_2	30/7/30	–	–	8	1	[40]
Cellophane	TiO_2/Au/TiO_2	30/10/40	9.5	82.1	86	14.6	[37]
PET	TiO_2:Nb/Ag/TiO_2:Nb	34/8/42	11.9	83	69	13	[36]
PET	NiO/Ag/NiO	42/8/72	16.4	74	45	3	[36]
PET	NiO/Ag/NiO	35/11/35	7.6	80	105[a]	14.1[a]	[38]
Glass	NiO/Ag/NiO	10/15/30	4.2	90	214	83	[45]
PET	Bi_2O_3/Au/Bi_2O_3	120/7/120	–	–	6	0.5	[40]
PET	MoO_3/Ag(film)/MoO_3	40/10/40	6.12	69.8	114.05[a]	4.47	[39]
PET	MoO_3/Ag(grid)/MoO_3	40/10/40	5.88	76.5	130.1[a]	11.6	[39]
PET	Zn:SnO_2/Ag/Zn:SnO_2	30/12/30	7.5	85	113.3[a]	26.25[a]	[46]

[a] Calculated from available data R_{sq} and T % from graphs.

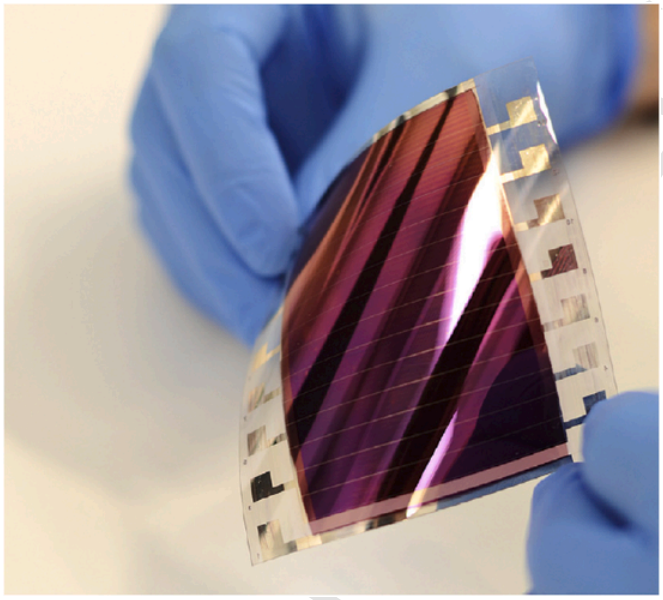

Fig. 5. Picture of flexible module using IMI (ITO/METAL/ITO) sputtered stack as a transparent electrode. Reprinted with the permission from Organic Electronics 15 (2014) 2256 [43].

layer sequence of all devices was: PET/ITO/Ag/ITO/AZO/P3HT:PCBM/PEDOT:PSS/Ag with a maximum efficiency of 3.3%, corresponding to a J_{sc} = 0.66 mA/cm^2, a V_{oc} = 8.13V and an FF = 61.60% under standard illumination of 1000W/m^2 Solar simulator with AM1.5G, for a module with a total surface of 70 mm × 50 mm (3500 mm^2).

In 2015, the first large-scale demonstration of fully solution coated, semitransparent, flexible organic photovoltaic modules deposited on PET using IMI electrodes was presented at the Universal Exhibition Milan (see Fig. 6).

The active layer of these cells is a polymer: fullerene blend (PBTZT-stat-BDTT-8:PCBM) and the efficiency of the modules PET/**ITO/Metal/ITO**/PEDOT:PSS/PBTZT-stat-BDTT-8:PCBM/Ag, with a surface of 114.5 cm^2 is around of 4.5% [47].

More recently (2021) the IMI multilayer structures were used as top electrodes for the manufacturing of semi-transparent perovskites solar cells deposited on PET substrate (see Fig. 7) [35].

An increase of the efficiency of perovskite solar cells using three layers oxide/metal/oxide electrodes PET/IZO/PTAA/PVK/C60/SnO_x/**ITO/Ag/ITO** (PCE = 9.02%) was remarked compared to the standard structure using a single layer ITO electrode PET/IZO/PTAA/PVK/C60/SnO_x/**ITO** (PCE = 7.96%), [35].

The studies of OPV and PVK solar cells using oxide/metal/oxide electrodes, in general, and in particular on flexible substrates are very limited up to now. In some cases, due to the lack of data, in the Table 4 here below, the performances of devices deposited on glass substrates are given as example in the case of some unique investigations, as for example for TiO_2/Ag/TiO_2 (TAT) electrodes for OPV solar cells or NiO/Ag/NiO (NAN) for PVK solar cells. Table 4 summarized the data collected from literature concerning the OPV and PVK solar cells deposited on PET or other flexible substrate using ITO/Metal/ITO (IMI), ZnO/Ag/ZnO (ZAZ), TiO_2/Ag/TiO_2 (TAT), NiO/Ag/NiO (NAN) or other DMD (dielectric/metal/dielectric) or OMO (oxide/metal/oxide) transparent electrodes. In fact, all these multilayer structures are DMD or OMO multilayers structures, but as it does not exist yet a unified admitted abbreviation, the one indicated in Table 4 corresponds to the abbreviation chosen by the majority of authors in their respective papers. Hence, the MoO_3/Au/MoO_3 electrodes are usually designated as DMD electrodes and not MAM as one can expected compared to the other multilayer structures mentioned previously. The performances of the devices using oxide/metal/oxide top or bottom electrodes, are compared (when these data are available) with the performances of the devices of the same se-

Fig. 6. Images of A) a commercial module fabricated by BELECTRIC OPV using ITO/Metal/ITO electrodes on plastic substrates B) chemical structure of the polymer used: PBTZT-stat-BDTT, and C) large scale deployment of BELECTRIC OPV modules at the Universal Exhibition Milan 2015. Reprinted with permission from Advanced Science 3 (2015) 1500342 [47].

ries in standard configurations. In this case, the variation of the efficiency (VAR PCE%) is given in the fifth column of solar cells performances after J_{sc}, V_{oc}, FF and PCE.

As one can see, the performances of the devices using oxide/metal/oxide electrodes are comparable to the standard ones. The usual relative variations in efficiency $(\eta_{\text{with OMO}} - \eta_{\text{standard}})/\eta_{\text{standard}}$ are of $\pm 25\%$.

For OPV Solar cells using NiO/Ag/NiO electrodes on PET substrates an increase of the efficiency from 4.42% for the classical architecture PET/**ITO**/PEDOT:PSS/PBDTT-C:PCBM/LiF/Al to 5.55% was obtained when ITO was replaced with an NAN electrode: PET/**NiO/Ag/NiO**/PBDTT-C:PCBM/LiF/Al. The I–V characteristics of these devices are given in Fig. 8 [38].

Another successful device is a PVK solar cell realized in 2019 by Hongjiang Li et all. of an ultra-flexible and biodegradable perovskite solar cells with an efficiency of 13% utilizing ultrathin cellophane paper substrates and **TiO_2/Ag/TiO_2** transparent electrodes (see Fig. 9).

Other recent research mentioned the manufacturing of flexible PVK solar cells using Titanium or paper substrates and MoO_x/Ag/MoO_x as top electrodes [48,49]. The efficiencies obtained for the devices deposited on Titanium foil were of 14.5% and for those on paper of 2.7%.

The interest of transparent oxide/metal/oxide electrodes increase constantly last year due also to their potential in the fabrication of semi-transparent solar cells and also as intermediate electrodes for tandem solar cells. However, until now the majority of existing data refers on devices deposited on glass substrates.

5. Conclusions

The present work offers a novel approach in successfully exploiting the oxide/metal/oxide as bottom or top electrodes for organic and perovskite solar cells.

The properties of different type of oxide/metal/oxide electrodes such as: ITO/Metal/ITO, ZnO/Au or Ag/ZnO, NiO/Ag/NiO, TiO2/Ag/TiO2, MoO3/Ag/MoO3, SnO2/Ag/SnO2 etc. are analyzed. The most promising materials and the best choices in term of layers thickness are identified for obtaining high quality electrodes. The solar cells performances using these three layer electrodes are compared with those of the same devices in the classical configuration using ITO or FTO on plastic substrates as bottom electrodes or Au and Ag silver as top electrodes.

The unique mechanical, optical and electrical properties of oxide/metal/oxide electrodes make them more suitable for the deposition on flexible substrates such as paper, cellophane, PET, recycled PET or other plastic substrates than the classical ITO or FTO films which are brittle and do not resist to bending, torsion or other mechanical stress. These properties associated with a highly efficient lightweight and flexible device, demonstrate that these new structures can replace easily

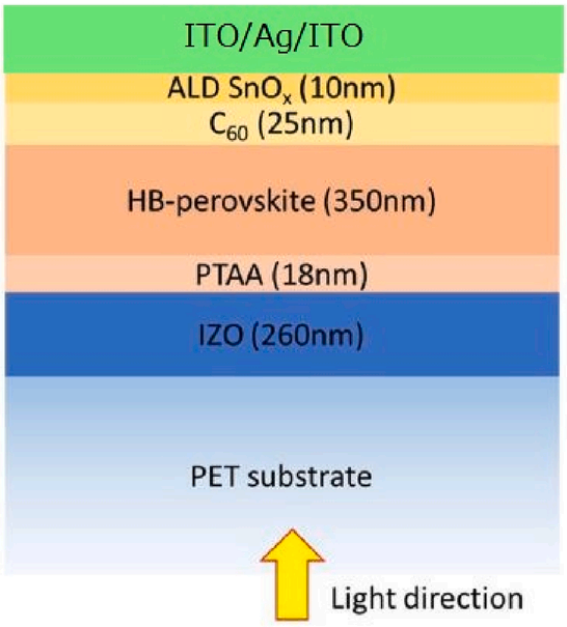

Fig. 7. Schematic of a **H**igh **B**andgap perovskite solar cell of p-i-n configuration on PET substrate with an ITO/Ag/ITO top electrode. Reprinted with permission from Applied Physics Letters 118 (2021) 241110-1 [35].

the classical ITO of FTO electrodes. This replacement will lead to the reduction or the suppression of a series of rare materials used for solar cells fabrication and also offers the possibility to use recycled materials or biodegradable materials as supports. Moreover, transparent conducting oxide/metal/oxide can also replace the Au or Ag top electrodes, opening hence the area for the development of a new class of solar cells, the one of semi-transparent organic and perovskites solar cells on flexible substrates.

CRediT authorship contribution statement

Mihaela Girtan: Conceptualization, Methodology, Formal analysis, Investigation, Data curation, Writing – original draft, review. **Beatrice Negulescu:** Investigation, instrumentation, analysis tools and visualisation, review editing.

Declaration of competing interest

The authors declare that they have no known competing financial interests or personal relationships that could have appeared to influence the work reported in this paper.

Acknowledgments

The authors are thankful to Romain Mallet, from SCIAM, Angers University for long date collaboration and for the analysis by Scanning electron Microscopy of some of samples presented in this article.

Table 4
OPV and PVK solar cells performances using oxide/metal/oxide electrodes in comparison with their characteristics in the classical (standard) configuration using ITO, IZO, FTO (bottom) or Ag, Au (top) electrodes.

Type of structure OMO or DMD vs. Standard configuration single ITO or FTO		Cell type	Cell architecture	Best solar cells performances compared to standard architecture					Year	Ref.
				J_{sc} (mA/cm^2)	V_{oc} (V)	FF (%)	PCE (%)	Var. PCE (%)		
IMI	ITO/Ag/ITO	OPV	PET/**ITO/Ag/ITO**/AZO/P3HT:PCBM/PEDOT:PSS/Ag (cell)	8.86	0.57	64.0	3.25	–	2014	
	ITO/Ag/ITO		PET/**ITO/Ag/ITO**/AZO/P3HT:PCBM/PEDOT:PSS/Ag (module)	0.66	8.13	61.6	3.3	–		
	ITO (Standard)		PET/**ITO**/AZO/P3HT:PCBM/PEDOT:PSS/Ag	–	–	–	–			
	ITO/Metal/ITO		PET/**ITO/Metal/ITO**/PEDOT:PSS/PBTZT-stat-BDTT-8:PCBM/Ag (cell)	12.6	0.77	67	6.5	–	2015	[47]
	ITO/Metal/ITO		PET/**ITO/Metal/ITO**/PEDOT:PSS/PBTZT-stat-BDTT-8:PCBM/Ag (module)	9.8	0.78	64	4.8	–		
	ITO (on glass)		glass/**ITO**/PEDOT:PSS/PBTZT-stat-BDTT-8:PCBM/Ag (cell)	14.3	0.8	68	7.5	–		
	ITO (Standard)		PET/**ITO**/PEDOT:PSS/PBTZT-stat-BDTT-8:PCBM/Ag	–	–	–	–			
	ITO/Ag/ITO	PVK	PET/IZO/PTAA/PVK/C60/SnOx/**ITO/Ag/ITO** (top electrode)	13.20	1.03	66.4	9.02	+13.3	2021	[35]
	ITO/Ag/Cu/ITO		PET/IZO/PTAA/PVK/C60/SnOx/**ITO/Ag/Cu/ITO** (top electrode)	13.70	1.03	63.1	8.91	+11.9		
	ITO (Standard)		PET/IZO/PTAA/PVK/C60/SnOx/**ITO**	13.20	1.04	57.9	7.96			
ZAZ	ZnO/Ag/ZnO	OPV	glass/**ZnO/Ag/ZnO**/MoO_3/P3HT:PCBM/Al	9.50	0.54	50.0	2.58	- 13.7	2013	[50]
	ITO (Standard)		glass/**ITO**/MoO_3/P3HT:PCBM/Al	10.90	0.54	51.0	2.99			
	ZnO/Ag/ZnO		PET/**ZnO/Ag/ZnO**/P3HT:PCBM/PEDOT:PSS/Ag	6.00	0.51	60.0	1.86	- 25.6	2014	[34]
	ITO (Standard)		PET/**ITO**/ZnO/P3HT:PCBM/PEDOT:PSS/Ag	8.30	0.52	58.0	2.50			
	ZnO/Ag/ZnO		PEN/**ZnO/Ag/ZnO**/PIDT-PhanQ:PCBM/MoO_3/Ag	11.00	0.87	64.0	6.04	+8.2	2014	[44]
	ITO (Standard)		PEN/**ITO**/PIDT-PhanQ:PCBM/MoO_3/Ag	11.90	0.82	57.0	5.58			
TAT	TiO_2/Ag/TiO_2	OPV	glass/**TiO_2/Ag/TiO_2**/PTB7:PCBM/PEDOT:PSS/Ag	17.54	0.76	65.8	8.70	+16	2015	[51]
	ITO (Standard)		glass/**ITO**/TiO_2/PTB7:PCBM/PEDOT:PSS/Ag	15.64	0.75	64.3	7.50			
	TiO_2/Ag/TiO_2		glass/**TiOx/Ag/TiOx**/ZnO/P3HT:PCBM/PEDOT:PSS/Ag	8.37	0.52	62.0	2.70	- 14.0	2016	[52]
	ITO (Standard)		glass/**ITO**/ZnO/P3HT:PCBM/PEDOT:PSS/Ag	9.17	0.53	63.0	3.14			
	TiO_2/Ag/TiO_2		glass/**TiO_2/Ag/TiO_2**/MoO_3/P3HT:PCBM/LiF/Al	8.78	0.51	49.0	2.18	+ 101.8	2016	[53]
	ITO (Standard)		glass/**ITO**/MoO_3/P3HT:PCBM//LiF/Al	6.04	0.44	44.0	1.08			
	TiO_2/Ag/TiO_2	PVK	cellophane/**TiO_2/Ag/TiO_2**/C60 pyrrolidinetris-acid (CPTA)/ CH3NH3PbI3/Spiro-OMeTAD/Au	17.75	1.04	70.0	13.00	–	2019	[37]
	TiO_2/Ag/TiO_2		glass/**TiO_2/Ag/TiO_2**/C60 pyrrolidinetris-acid (CPTA)/ CH3NH3PbI3/Spiro-OMeTAD/Au	19.80	1.04	72.0	14.88	–		
	FTO (Standard)		cellophane/FTO/**TiO_2**/C60 pyrrolidinetris-acid (CPTA)/ CH3NH3PbI3/Spiro-OMeTAD/Au	–	–	–	–			
NAN	NiO/Ag/NiO	OPV	glass/**NiO/Ag/NiO**/PBDTT-C:PCBM/LiF/Al	13.37	0.71	64.0	6.07	+2.8	2014	[38]
	ITO (standard)		glass/**ITO**/PEDOT:PSS/PBDTT-C:PCBM/LiF/Al	13.92	0.70	61.0	5.90			
	NiO/Ag/NiO		PET/**NiO/Ag/NiO**/PBDTT-C:PCBM/LiF/Al	12.91	0.71	61.0	5.55	+25.5		
	ITO (standard)		PET/**ITO**/PEDOT:PSS/PBDTT-C:PCBM/LiF/Al	13.20	0.70	48.0	4.42			
	NiO/Ag/NiO	PVK	glass/FTO/TiO_2/CH3NH3PbI3/SpiroOMeTAD/**NiO/Ag/NiO** (top electrode)	19.96	1.06	73.1	15.80	- 13.1	2018	[45]
	NiO/Ag/NiO		glass/Eu(TTA)$_2$(Phen)MAA/FTO/TiO_2/CH3NH3PbI3/ SpiroOMeTAD/**NiO/Ag/NiO**/Lantanides doped NaYF4/Ag (intermediate electrode in tandem solar cells)	27.10	–	–	19.50	+7.1		
	Au (standard)		glass/FTO/TiO_2/CH3NH3PbI3/SpiroOMeTAD/**Au**	22.60	1.07	74.7	18.20			
	NiO/Ag/NiO		glass/ITO/**NiO/Ag/NiO**/MAPbI3/C_{70}/BCP/Ag (hole transport layer)	20.07	0.94	61.9	11.68	+5.9	2020	[54]
	NiO (standard)		glass/ITO/**NiO**/MAPbI3/C_{70}/BCP/Ag (hole transport layer	19.45	0.94	60.3	11.02			
	NiO/Ag/NiO		glass/ITO/**NiO/Ag/NiO**/FA_xMA_{1-x}/C_{70}/BCP/Ag (hole transport layer)	22.97	0.95	58.1	12.67	–		
	NiO (standard)		(hole transport layer)	–	–	–	–			
DMD (OMO)	MoO_3/Au/MoO_3	OPV	glass/Al/ZnO-np/P3HT:PCBM/**MoO_3/Au/MoO_3** (top electrode)	6.70	0.59	63.0	2.50	- 19.3	2012	[55]
	MoO_3/Au/MoO_3		PET/Al/ZnO-np/P3HT:PCBM/**MoO_3/Au/MoO_3** (top electrode)	6.50	0.60	62.0	2.40	- 22.5		
	MoO_3/Ag/MoO_3		glass/Al/ZnO-np/P3HT:PCBM/**MoO_3/Ag/MoO_3** (top electrode)	5.50	0.59	61.0	2.00	- 35.4		
	ITO & MoO_3/Al (standard)		glass/**ITO**/ZnO-np/P3HT:PCBM/**MoO_3/Al**	8.10	0.62	61.0	3.10			
	MoO_3/Ag/MoO_3		PET/**MoO_3/Ag/MoO_3**/P3HT:PCBM/Ca/Ag	6.63	0.63	64	2.50		2015	[56]
	ITO (standard)		PET/ITO/P3HT:PCBM/Ca/Ag	–	–	–	–			
	MoO_3/Ag/MoO_3		glass/**MoO_3/Ag/MoO_3**/P3HT:PCBM/Ca/Ag	6.21	0.64	64	2.71	- 4.9		
	ITO (standard)		glass/ITO/P3HT:PCBM/Ca/Ag	–	–	–	2.85			
	MoO_3/Ag/MoO_3		glass/ITO/Alq_3/C_{60}/SubPc/**MoO_3/Ag/MoO_3** (top electrode)	5.04	0.94	48.0	2.34	- 22	2021	[57]
	MoO_3/Al (standard)		glass/ITO/Alq_3/C_{60}/SubPc/**MoO_3/Al** (top electrode)	5.60	0.94	57.0	3.00			

(*continued on next page*)

Table 4 (*continued*)

Type of structure OMO or DMD vs. Standard configuration single ITO or FTO		Cell type	Cell architecture	Best solar cells performances compared to standard architecture					Year	Ref.
				J_{sc} (mA/cm^2)	V_{oc} (V)	FF (%)	PCE (%)	Var. PCE (%)		
	MoO_3/Au/MoO_3	PVK	glass/FTO/CH3NH3PbI3/SpiroOMeTAD/**MoO_3/Au/MoO_3** (top electrode)	20.40	0.98	58.0	13.60	–	2015	[41]
	Au (standard)		glass/FTO/CH3NH3PbI3/SpiroOMeTAD/**Au**	–	–	–	–			
	MoO_x/Ag/Au/MoO_x		glass/ITO/TiO_x/CH3NH3PbI3/Spiro-OMeTAD/**MoO_x/Ag/Au/MoO_x** (top electrode)	14.6	1.05	75.1	11.5	- 30	2015	[58]
	Au (standard)		glass/ITO/TiO_x/CH3NH3PbI3/Spiro-OMeTAD/**Au**	21.10	1.07	73.4	16.5			
	MoO_3/Au/Ag/MoO_3		NOA63 (polymer)/MoO_3/Au/PEDOT:PSS/CH3NH3PbI3/PCBM/**MoO_3/Au/Ag/MoO_3**/Alq_3	14.67	0.94	62.3	8.60	–	2016	[59]
	MoO_3/Au/Ag/MoO_3		NOA63 (polymer)/ITO/PEDOT:PSS/CH3NH3PbI3/PCBM/**MoO_3/Au/Ag/MoO_3**/Alq_3	18.21	0.94	70.0	12.02	–		
	Au (standard)		NOA63(polymer)/ITO/PEDOT:PSS/CH3NH3PbI3/PCBM/**Au**	–	–	–	–			
	MoO_x/Ag/MoO_x		glass/FTO/TiO_2/CH3NH3PbI3/Spiro-OMeTAD/**MoO_x/Ag/MoO_x** (top electrode)	18.29	1.00	68.0	12.45	–	2019	[49]
	MoO_x/Ag/MoO_x		Ti foil/TiO_2/CH3NH3PbI3/Spiro-OMeTAD/**MoO_x/Ag/MoO_x** (top electrode)	18.1	1.07	75.0	14.5	–		
	Au (standard)		glass/FTO/TiO_2/CH3NH3PbI3/Spiro-OMeTAD/**Au**	–	–	–	–			
DMD	SnO_x/Ag/SnO_x	OPV	glass/ITO/PEDOT:PSS/CH3NH3PbI3/PCBM/AZO/**SnOx/Ag/SnOx**	11.2	0.86	73.0	11.2	+12	2017	[60]
	Ag (standard)		glass/ITO/PEDOT:PSS/CH3NH3PbI3/PCBM/AZO/**Ag**	10	0.84	70.2	10			

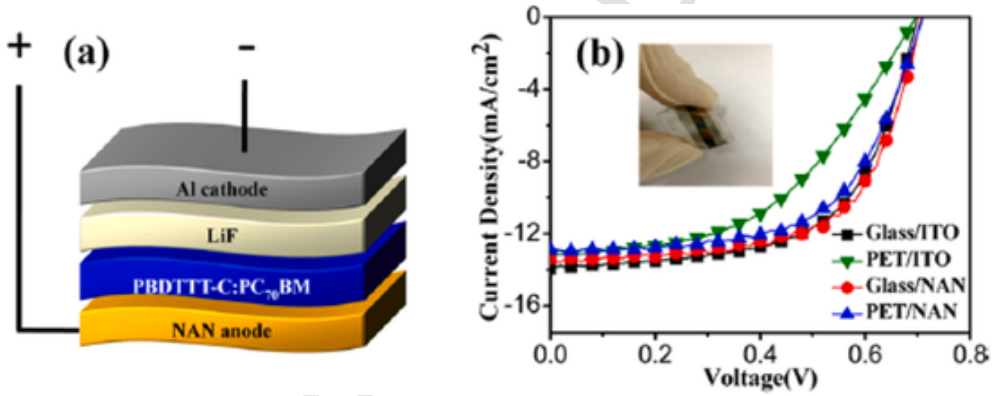

Fig. 8. (a) The architecture and (b) the I–V characteristics of an OPV solar cells using NiO/Ag/NiO electrodes on PET substrates. Reprinted with permission from ACS Applied Materials and Interfaces 6 (2014) 16403 [38].

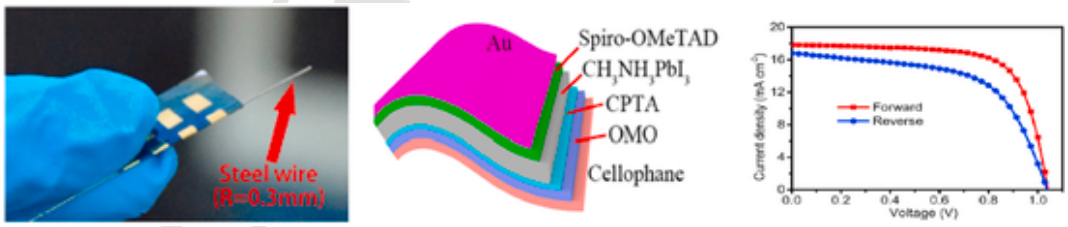

Fig. 9. PVK solar cell on cellophane substrate having the following architecture: cellophane/**TiO_2/Ag/TiO_2**/C60 pyrrolidinetris-acid (CPTA)/CH3NH3PbI3/Spiro-OMeTAD/Au. Reprinted with permission from Solar Energy 188 (2019) 158 [37].

References

[1] Mihaela Girtan, Future Solar Energy Devices, Springer, 2018, [Online]. Available:. https://www.springer.com/gp/book/9783319673363.

[2] M. Girtan, Is photonics the new electronics? Mater. Today 17 (3) (2014) 100–101, https://doi.org/10.1016/j.mattod.2014.03.003.

[3] M. Girtan, New trends in solar cells research, SpringerBriefs.Appl. Sci. Technol. 9783319673363 (2018) 45–75, https://doi.org/10.1007/978-3-319-67337-0_3.

[4] A. Chiasera, et al., Flexible photonics: transform rigid materials into mechanically flexible and optically functional systems, in: Proceedings of SPIE - the International Society for Optical Engineering, vol. 11682, 2021, https://doi.org/10.1117/12.2577860.

[5] G. Canazza, F. Scotognella, G. Lanzani, S. De Silvestri, M. Zavelani-Rossi, D. Comoretto, Lasing from all-polymer microcavities, Laser Phys. Lett. 11 (3) (2014), https://doi.org/10.1088/1612-2011/11/3/035804.

[6] F. Scotognella, A. Monguzzi, F. Meinardi, R. Tubino, DFB laser action in a flexible fully plastic multilayer, Phys. Chem. Chem. Phys. 12 (2) (2010) 337–340, https://doi.org/10.1039/b917630f.

[7] G. C. Righini, J. Krzak, A. Lukowiak, G. Macrelli, S. Varas, and M. Ferrari, "From flexible electronics to flexible photonics: a brief overview," Opt. Mater., vol. 115, 2021, doi: 10.1016/j.optmat.2021.111011.

[8] F. Marangi, M. Lombardo, A. Villa, F. Scotognella, New strategies for solar cells beyond the visible spectral range, Opt. Mater. X 11 (2021), https://doi.org/10.1016/j.omx.2021.100083.

[9] A. Radu, et al., The influence of lif layer and ZnO nanoparticles addings on the performances of flexible photovoltaic cells based on polymer blends, Digest.J. Nanomater.Biostructures 6 (3) (2011) 1141–1148.

[10] A. Stanculescu, M. Socol, G. Socol, I.N. Mihailescu, M. Girtan, F. Stanculescu,

Maple prepared organic heterostructures for photovoltaic applications, Appl. Phys. Mater. Sci. Process 104 (3) (2011) 921–928, https://doi.org/10.1007/s00339-011-6440-y.
[11] K.-J. Ko et al., "Fabrication of an oxide/metal/oxide structured electrode integrated with antireflective film to enhance performance in flexible organic light-emitting diodes," Materials Today Energy, vol. 20, 2021, doi: 10.1016/j.mtener.2021.100704.
[12] M. Girtan, A. Wittenberg, M.L. Grilli, D.P.S. de Oliveira, C. Giosuè, M.L. Ruello, The critical raw materials issue between scarcity, supply risk, and unique properties, Materials 14 (8) (2021), https://doi.org/10.3390/ma14081826.
[13] A. Rane, A.R. Ajitha, M.K. Aswathi, P. Manju, K. Kanny, S. Thomas, 9 - applications of waste poly(ethylene terephthalate) bottles, in: S. Thomas, A. Rane, K. Kanny, A. V.K, M.G. Thomas (Eds.), Recycling of Polyethylene Terephthalate Bottles, William Andrew Publishing, 2019, pp. 169–189, https://doi.org/10.1016/B978-0-12-811361-5.00009-2.
[14] C.G. Granqvist, Transparent conductors as solar energy materials: a panoramic review, Sol. Energy Mater. Sol. Cell. 91 (17) (2007) 1529–1598.
[15] C.G. Granqvist, Solar energy materials, Adv. Mater. 15 (21) (2003) 1789–1803.
[16] C.G. Granqvist, Transparent conductors for solar energy and energy efficiency: a broad-brush picture, Int. J. Nanotechnol. 6 (9) (2009) 785–798.
[17] A. Stanculescu et al., "Effect of ITO electrode patterning on the properties of organic heterostructures based on non-fullerene acceptor prepared by MAPLE," Appl. Surf. Sci., vol. 509, 2020, doi: 10.1016/j.apsusc.2020.145351.
[18] M. Girtan, A. Bouteville, G.G. Rusu, M. Rusu, Preparation and properties of SnO2: F thin films, J. Optoelectron. Adv. Mater. 8 (1) (2006) 27–30.
[19] P. Koralli, S.F. Varol, M. Kompitsas, M. Girtan, Brightness of blue/violet luminescent nano-crystalline AZO and IZO thin films with effect of layer number: for high optical performance, Chin. Phys. Lett. 33 (5) (2016), https://doi.org/10.1088/0256-307X/33/5/056801.
[20] M. Socol, et al., Organic heterostructures deposited by MAPLE on AZO substrate, Appl. Surf. Sci. 417 (2017) 196–203, https://doi.org/10.1016/j.apsusc.2017.02.260.
[21] A. Stanculescu, et al., MAPLE prepared heterostructures with oligoazomethine: fullerene derivative mixed layer for photovoltaic applications, Appl. Surf. Sci. 417 (2017) 183–195, https://doi.org/10.1016/j.apsusc.2017.03.053.
[22] F. Ghomrani, et al., Influence of Al doping agents nature on the physical properties of Al: ZnO films deposited by spin-coating technique, Optoelectron. Adv. Mater.Rapid Commun. 5 (3) (2011) 247–251.
[23] S. Iftimie, R. Mallet, J. Merigeon, L. Ion, M. Girtan, S. Antohe, On the structural, morphological and optical properties of ITO, ZnO, ZnO:Al and NiO thin films obtained by thermal oxidation, Digest.J. Nanomater.Biostructures 10 (1) (2015) 221–229.
[24] M. Girtan, M. Socol, B. Pattier, M. Sylla, A. Stanculescu, On the structural, morphological, optical and electrical properties of sol-gel deposited ZnO:In films, Thin Solid Films 519 (2) (2010) 573–577, https://doi.org/10.1016/j.tsf.2010.07.006.
[25] M. Girtan, M. Kompitsas, M. Kompitsas, I. Fasaki, On physical properties of undoped and Al and in doped zinc oxide films deposited on PET substrates by reactive pulsed laser deposition, EPJ Applied Physics 51 (3) (2010), https://doi.org/10.1051/epjap/2010112, 33212-p1-33212-p.5.
[26] M. Girtan, Theoretical aspects of materials physics, SpringerBriefs.Appl. Sci. Technol. 9783319673363 (2018) 15–44, https://doi.org/10.1007/978-3-319-67337-0_2.
[27] M. Girtan, R. Mallet, M. Socol, A. Stanculescu, On the physical properties PEDOT: PSS thin films, Materials Today Communications 22 (2020), https://doi.org/10.1016/j.mtcomm.2019.100735.
[28] M. Girtan, R. Mallet, D. Caillou, G.G. Rusu, M. Rusu, Thermal stability of poly(3, 4-ethylenedioxythiophene)-polystyrenesulfonic acid films electrical properties, Superlattice. Microst. 46 (1–2) (2009) 44–51.
[29] W. Cao, J. Li, H. Chen, J. Xue, Transparent electrodes for organic optoelectronic devices: a review, J. Photon. Energy 4 (1) (2014) 1–28, https://doi.org/10.1117/1.JPE.4.040990.
[30] M. Zhang, et al., Single-layered organic photovoltaics with double cascading charge transport pathways: 18% efficiencies, Nat. Commun. 12 (1) (Jan. 2021) 309, https://doi.org/10.1038/s41467-020-20580-8.
[31] J. Jeong, et al., Pseudo-halide anion engineering for α-FAPbI3 perovskite solar cells, Nature 592 (7854) (Apr. 2021) 381–385, https://doi.org/10.1038/s41586-021-03406-5.
[32] M. Girtan, L. Hrostea, M. Boclinca, B. Negulescu, Study of oxide/metal/oxide thin films for transparent electronics and solar cells applications by spectroscopic ellipsometry, AIMS Materials Science 4 (3) (2017) 594–613, https://doi.org/10.3934/matersci.2017.3.594.
[33] M. Girtan, Comparison of ITO/metal/ITO and ZnO/metal/ZnO characteristics as transparent electrodes for third generation solar cells, Sol. Energy Mater. Sol. Cell. 100 (2012) 153–161, https://doi.org/10.1016/j.solmat.2012.01.007.
[34] A. El Hajj, T.M. Kraft, B. Lucas, M. Schirr-Bonnans, B. Ratier, P. Torchio, Flexible inverted polymer solar cells with an indium-free tri-layer cathode, J. Appl. Phys. 115 (3) (2014), https://doi.org/10.1063/1.4861171.
[35] P. Spinelli, R. Fuentes Pineda, M. Scigaj, T. Ahmad, K. Wojciechowski, Transparent conductive electrodes based on co-sputtered ultra-thin metal layers for semi-transparent perovskites solar cells, Appl. Phys. Lett. 118 (24) (2021), https://doi.org/10.1063/5.0052209.
[36] L. Hrostea, P. Lisnic, R. Mallet, L. Leontie, M. Girtan, Studies on the physical properties of TiO2:Nb/Ag/TiO2:Nb and NiO/Ag/NiO three-layer structures on glass and plastic substrates as transparent conductive electrodes for solar cells, Nanomaterials 11 (2021) 6, https://doi.org/10.3390/nano11061416.
[37] H. Li, et al., Ultraflexible and biodegradable perovskite solar cells utilizing ultrathin cellophane paper substrates and TiO2/Ag/TiO2 transparent electrodes, Sol. Energy 188 (2019) 158–163, https://doi.org/10.1016/j.solener.2019.05.061.
[38] Z. Xue, et al., High-performance NiO/Ag/NiO transparent electrodes for flexible organic photovoltaic cells, ACS Appl. Mater. Interfaces 6 (18) (2014) 16403–16408, https://doi.org/10.1021/am504806k.
[39] C.-T. Wang, C.-C. Ting, P.-C. Kao, S.-R. Li, S.-Y. Chu, Improvement of optical and electric characteristics of MoO3/Ag film/MoO3 flexible transparent electrode with metallic grid, J. Appl. Phys. 120 (19) (2016), https://doi.org/10.1063/1.4968011.
[40] L. Hrostea, M. Boclinca, M. Socol, L. Leontie, A. Stanculescu, M. Girtan, Oxide/metal/oxide electrodes for solar cell applications, Sol. Energy 146 (2017) 464–469, https://doi.org/10.1016/j.solener.2017.03.017.
[41] E. Della Gaspera, et al., Ultra-thin high efficiency semitransparent perovskite solar cells, Nano Energy 13 (2015) 249–257, https://doi.org/10.1016/j.nanoen.2015.02.028.
[42] M. Girtan, R. Mallet, On the electrical properties of transparent electrodes, Proc. Rom. Acad. Math. Phys. Tech. Sci. Inf. Sci. 15 (2) (2014) 146–150.
[43] P. Kubis, et al., High precision processing of flexible P3HT/PCBM modules with geometric fill factor over 95%, Org. Electron. 15 (10) (2014) 2256–2263, https://doi.org/10.1016/j.orgel.2014.06.006.
[44] J. Zou, C.-Z. Li, C.-Y. Chang, H.-L. Yip, A.K.-Y. Jen, Interfacial engineering of ultrathin metal film transparent electrode for flexible organic photovoltaic cells, Adv. Mater. 26 (22) (2014) 3618–3623, https://doi.org/10.1002/adma.201306212.
[45] H. Li, et al., Near-infrared and ultraviolet to visible photon conversion for full spectrum response perovskite solar cells, Nano Energy 50 (2018) 699–709, https://doi.org/10.1016/j.nanoen.2018.06.024.
[46] Y. Cho, N.S. Parmar, S. Nahm, J.-W. Choi, Full range optical and electrical properties of Zn-doped SnO2and oxide/metal/oxide multilayer thin films deposited on flexible PET substrate, J. Alloys Compd. 694 (2017) 217–222, https://doi.org/10.1016/j.jallcom.2016.09.293.
[47] S. Berny, et al., Solar trees: first large-scale demonstration of fully solution coated, semitransparent, flexible organic photovoltaic modules, Advanced Science 3 (5) (2015), https://doi.org/10.1002/advs.201500342.
[48] J. Long, Z. Huang, J. Zhang, X. Hu, L. Tan, Y. Chen, Flexible perovskite solar cells: device design and perspective, Flexible and Printed Electronics 5 (1) (2020), https://doi.org/10.1088/2058-8585/ab556e.
[49] G.S. Han, et al., Multi-functional transparent electrode for reliable flexible perovskite solar cells, J. Power Sources 435 (2019), https://doi.org/10.1016/j.jpowsour.2019.226768.
[50] S. Vedraine, A. El Hajj, P. Torchio, B. Lucas, Optimized ITO-free tri-layer electrode for organic solar cells, Org. Electron. 14 (4) (2013) 1122–1129, https://doi.org/10.1016/j.orgel.2013.01.030.
[51] K.-D. Kim, et al., Decoupling optical and electronic optimization of organic solar cells using high-performance temperature-stable TiO2/Ag/TiO2 electrodes, Apl. Mater. 3 (2015) 10, https://doi.org/10.1063/1.4933414.
[52] A. Bou, et al., Optical role of the thin metal layer in a TiOx/Ag/TiOx transparent and conductive electrode for organic solar cells, RSC Adv. 6 (109) (2016) 108034–108044, https://doi.org/10.1039/c6ra22081a.
[53] Z. Zhao, T.L. Alford, The optimal TiO2/Ag/TiO2 electrode for organic solar cell application with high device-specific Haacke figure of merit, Sol. Energy Mater. Sol. Cell. 157 (2016) 599–603, https://doi.org/10.1016/j.solmat.2016.07.044.
[54] K.-C. Chang, T.-H. Yeh, H.-Y. Lee, C.-T. Lee, High performance perovskite solar cells using multiple hole transport layer and modulated FAxMA1−xPbI3 active layer, J. Mater. Sci. Mater. Electron. 31 (5) (2020) 4135–4141, https://doi.org/10.1007/s10854-020-02961-3.
[55] W. Cao, Y. Zheng, Z. Li, E. Wrzesniewski, W.T. Hammond, J. Xue, Flexible organic solar cells using an oxide/metal/oxide trilayer as transparent electrode, Org. Electron. 13 (11) (2012) 2221–2228, https://doi.org/10.1016/j.orgel.2012.05.047.
[56] Z. Wang, et al., Flexible ITO-free organic solar cells based on MoO3/Ag anodes, IEEE Photonics Journal 7 (1) (2015), https://doi.org/10.1109/JPHOT.2015.2396906.
[57] L. Cattin, G. Louarn, M. Morsli, J.C. Bernède, Semi-transparent organic photovoltaic cells with dielectric/metal/dielectric top electrode: influence of the metal on their performances, Nanomaterials 11 (2) (2021) 1–10, https://doi.org/10.3390/nano11020393.
[58] Y. Yang Michael, et al., Multilayer transparent top electrode for solution processed perovskite/Cu(in,Ga)(Se,S)2 four terminal tandem solar cells, ACS Nano 9 (7) (2015) 7714–7721, https://doi.org/10.1021/acsnano.5b03189.
[59] X.-L. Ou, M. Xu, J. Feng, H.-B. Sun, Flexible and efficient ITO-free semitransparent perovskite solar cells, Sol. Energy Mater. Sol. Cell. 157 (2016) 660–665, https://doi.org/10.1016/j.solmat.2016.07.010.
[60] J. Zhao, et al., Self-encapsulating thermostable and air-resilient semitransparent perovskite solar cells, Adv. Energy Mater. 7 (2017) 14, https://doi.org/10.1002/aenm.201602599.